

# In Vitro 3D Model of Human Endometrial Stromal and Trophoblast Cells: Techniques for an Optimized Formation and Cryopreservation of Spheroids

Karthika Muthuraj, Iwona Scheliga, Dunja M. Baston-Buest, Jana Bender-Liebenthron, Jan-Steffen Kruessel, Alexandra P. Bielfeld

Article - Version of Record

Suggested Citation:

Muthuraj, K., Scheliga, I., Baston-Büst, D., Bender-Liebenthron, J., Krüssel, J.-S., & Bielfeld, A. P. (2026). In Vitro 3D Model of Human Endometrial Stromal and Trophoblast Cells: Techniques for an Optimized Formation and Cryopreservation of Spheroids. *Methods and Protocols* M&Ps, 9(1), Article 27. <https://doi.org/10.3390/mps9010027>

Wissen, wo das Wissen ist.

This version is available at:

URN: <https://nbn-resolving.org/urn:nbn:de:hbz:061-20260608-115742-3>

Terms of Use:

This work is licensed under the Creative Commons Attribution 4.0 International License.

For more information see: <https://creativecommons.org/licenses/by/4.0>

## Article

# In Vitro 3D Model of Human Endometrial Stromal and Trophoblast Cells: Techniques for an Optimized Formation and Cryopreservation of Spheroids

Karthika Muthuraj \*, Iwona Scheliga , Dunja M. Baston-Buest , Jana Bender-Liebenthron, Jan-Steffen Kruessel  and Alexandra P. Bielfeld 

Department of Obstetrics/Gynaecology and Reproductive Medicine, UniKiD Center for Reproductive Medicine (UniKiD), Medical Faculty and University Hospital Duesseldorf, Heinrich Heine University, Universitätsstraße 1, 40225 Duesseldorf, Germany

\* Correspondence: karthika.muthuraj@med.uni-duesseldorf.de

## Abstract

Three-dimensional (3D) cell culture models provide physiologically relevant systems that mimic the native endometrial environment better than 2D models and offer reliable platforms to study embryo implantation and maternal–embryo interactions. One widely used 3D culture model is the generation of spheroids. However, standardized and reproducible methods for generating uniform spheroids from trophoblast and endometrial stromal cells are limited. In this study, we established and validated a robust protocol for spheroid formation using human trophoblast (HTR8/SVneo, JEG3) and endometrial stromal (St-T1b, tHESC) cell lines. The protocol was further extended to generate spheroids from decidualized tHESC, representing a novel approach that closely reflects the receptive endometrial environment. Key parameters, including cell concentration and methyl cellulose supplementation, were optimized to produce compact and homogeneous spheroids. Spheroid formation was monitored at defined intervals (0, 8, 24, 32, and 48 h), and decidualized spheroids were assessed up to 72 h. Long-term cryopreservation over 11 months demonstrated high post-thaw viability across all spheroid types, as confirmed by Calcein-AM staining. This standardized workflow provides a reliable 3D model incorporating hormonally primed stromal cells and offers a practical platform to investigate the mechanisms underlying normal and trophoblast invasion in vitro.

**Keywords:** 3D spheroid model; methyl cellulose; freezing of spheroids; decidualized spheroids; post-thaw viability



Academic Editor: Jungyul Park

Received: 23 December 2025

Revised: 3 February 2026

Accepted: 9 February 2026

Published: 13 February 2026

**Copyright:** © 2026 by the authors.

Licensee MDPI, Basel, Switzerland.

This article is an open access article distributed under the terms and

conditions of the [Creative Commons Attribution \(CC BY\) license](https://creativecommons.org/licenses/by/4.0/).

## 1. Introduction

Three-dimensional (3D) cell culture systems such as spheroids and organoids have emerged as valuable in vitro models that more closely resemble the physiological cellular architecture, and its functionality as compared to two-dimensional (2D) monolayer culture [1]. 3D spheroid models, which are physiologically relevant, are widely used to study intracellular communication, and the microenvironment of in vivo tissues which has led to their widespread applications in drug screening [1], regenerative medicine [2], and reproductive biology [3]. The formation of a 3D spheroid is accomplished by various methods, namely the hanging drop model, spinner flask cultures, hydrogels, the liquid lay technique, and low attachment microwell plate techniques [4], among which the hanging drop model is a cost-effective robust method for producing uniform spheroids [5]. Irrespective of its

advantages, it has its limitations, especially due to the mono-layering of cells lacking to form spheroids as some cell lines need a more stable environment, e.g., the addition of methyl cellulose (MC). It is used to provide the matrix which supports the cells to form a stable 3D mass [6]. Parameters such as cell density, the medium used, and the concentration of additives can significantly influence the spheroid formation shape in a timely manner. Optimization of these factors is critical for generating uniform and viable spheroids suitable for downstream applications [7]. In reproductive biology, endometrial stromal (ES) cells (THESC [8], St-T1b [9]) and trophoblast cell lines (JEG3, HTR8/SVneo, Bewo, JAR [10]) are commonly used in *in vitro* models to study the early implantation process [10–12], trophoblast invasion [10], and embryo–maternal interactions [13]. However, though studies with 3D systems as a model for implantation and embryo–maternal interactions are increasing, standard spheroid formation protocols and systematic studies focusing on the formation and long-term preservation of spheroids are limited. While existing protocols for spheroid cryopreservation often rely on specialized cryoprotective agents [14–17], simple freezing approaches that could enable long-term storage, experimental reproducibility and logistical flexibility, remain largely unexplored. To the best of our knowledge, no previous study has reported the successful long-term freezing of trophoblast or stromal cell-derived spheroids using a simple freezing medium.

In this study, we aimed to investigate the impact of parameters such as cell concentration and MC supplementation on spheroid formation using a human endometrial stromal cell line (tHESC) and an immortalized decidual stromal cell line (St-T1b), as well as a first trimester extravillous trophoblast cell line (HRT8) and JEG3 choriocarcinoma cells derived from placental trophoblast. To better resemble the *in vivo* environment, we explored the spheroid-forming potential of decidualized tHESC (D-tHESC) cells for the first time. Decidualization is the functional differentiation of ES cells, that allows a competent embryo to implant into the uterus and thus serves also as a natural biomarker for successful implantation [18]. Decidualized stromal cells have been widely used in 2D monolayer cultures [19,20] for trophoblast invasion studies, whereas the formation of 3D spheroids from decidualized stromal cells as an *in vitro* model of the maternal endometrium, which more closely mimics the *in vivo* situation [21], has not been well characterized. Conditions such as cell concentration and MC content were investigated in the spheroid formation of D-tHESC cells. Following spheroid formation, we investigated the feasibility of using a simple and widely used freezing protocol to store spheroids and to subsequently assess their viability and morphology post-thawing. Taken together, these findings provide a comprehensive framework for generating and preserving viable spheroids from cell lines commonly used in implantation and pregnancy studies.

## 2. Materials and Methods

### 2.1. Cell Lines and Culture Conditions

Four human cell lines were utilized for spheroid formation: two endometrial stromal (ES) cell lines, namely tHESC (ATCC<sup>®</sup> CRL-4003<sup>™</sup>, Manassas, VA, USA) and the immortalized human endometrial cell line St-T1b, derived from first trimester decidual tissue (a generous gift from Professor Brosens, University of Warwick, Coventry, UK [22]). Two trophoblast cell lines, JEG3 (ATCC<sup>®</sup> HTB-36<sup>™</sup>, [23]), and HTR8/SVneo cells (ATCC<sup>®</sup> CRL3271<sup>™</sup>, [24]), were used. The tHESC, St-T1b and HTR8/SVneo cells were cultured in Dulbecco's Modified Eagle Medium (DMEM) supplemented with 7.5% fetal bovine serum (FBS), 1% penicillin-streptomycin (P/S), 100 mM sodium pyruvate, 7.5% sodium bicarbonate, 0.1% gentamycin (all from Biowest, Nuaille, France), and 0.04% insulin (Sigma-Aldrich/Merck, Darmstadt, Germany). JEG3 cells were maintained in Ham's F12 medium (Biowest, Nuaille, France) supplemented with 10% FBS and 1% P/S.

Endometrial cells were cultured in standard 100 mm cell culture dishes (Greiner Bio-One GmbH, Frickenhausen, Germany) and trophoblast cells were cultured in T75 cell culture flasks (CellStar<sup>®</sup>—Greiner Bio-One GmbH, Frickenhausen, Germany) at 37 °C in a humidified atmosphere containing 5% CO<sub>2</sub> (Binder GmbH, Tuttlingen, Germany). The culture medium was refreshed every 48 h and cells were passaged upon reaching approximately 80% confluence. For passaging, stromal and trophoblast cells were detached using 0.05% trypsin/EDTA (Biowest, Nuaille, France) prior to further experimental use.

## 2.2. Decidualization of Endometrial Stromal Cells—St-T1b and tHESC

Once the endometrial cells reached approximately 80% confluence, they were incubated with decidualization media as previously described [25]. Briefly, 0.5 mM 8-Br-cAMP (Biolog, Bremen, Germany) and 1 µM MPA (Sigma-Aldrich/Merck, Darmstadt, Germany) were added to DMEM medium (Biowest, Nuaille, France). This treatment was applied on days 1, 4, and continued up to day 7. Supernatants were collected on day 1 (pre-decidualization, negative control), day 4, and day 7, and analyzed for prolactin using an enzyme-linked immunosorbent assay (PRL-ELISA, R&D Systems, Minneapolis, MN, USA) following the manufacturer's instructions. Absorbance was measured at 450 nm using a microplate reader (Infinite F50, Tecan Trading AG, Männerdorf, Switzerland), and concentrations were calculated from a prolactin standard curve.

## 2.3. Spheroid Formation by the Hanging Drop Model

Spheroid formation was first optimized using tHESC and JEG3, investigating the spheroid development capacity by applying different cell concentrations, namely 20,000 cells/drop (higher) and 2000 cells/drop (lower), along with and without MC supplementation. Once the ideal conditions were established, the same protocol was extended to the St-T1b and HTR8/SVneo to evaluate its reproducibility across other physiologically relevant cell types.

Cell concentration in the suspension was determined using a hemocytometer (Labtech, Rotherham, UK). A 1.2% of MC stock solution (Sigma-Aldrich/Merck, Darmstadt, Germany) was prepared in the appropriate medium for each cell line [26]. The cell pellet was resuspended in a calculated volume of medium containing 25% of MC in order to prevent monolayer formation and promote a stable 3D spheroid development. The stromal cell lines t-HESC (both decidualized and non-decidualized) and JEG3 cells were tested with two different concentrations ranging from a lower (2000 cells/drop) to a higher cell count (20,000 cells/drop) and with/without MC using the hanging drop model. Spheroids were generated by dispensing 30 µL drops of the cell suspension to the lid of the 100 mm cell culture dish (Greiner Bio-One GmbH, Frickenhausen, Germany). The lid was carefully inverted over a phosphate-buffered saline (PBS; Biowest, Nuaille, France) filled base to maintain humidity and incubated at 37 °C with 5% CO<sub>2</sub> for 48 h. The D-tHESC spheroids were prepared in the same way but cultured in the hanging drop model for 72 h with an additional vigorous vortexing step prior to cell counting and seeding for the hanging drop model. This additional vortexing step was performed to minimize cell aggregation, as decidualized cells tend to form adherent sheet-like layers in suspension due to phenotypic and morphological changes associated with decidualization. Vortexing helped disrupt these layers and promote a more uniform single-cell distribution. Notably, even after vortexing, D-tHESC cells rapidly re-formed adherent layers; therefore, only the homogeneous liquid phase of the suspension, excluding visible cell layers, was carefully collected for cell counting and subsequent drop formation.

Finally, the following concentrations were used for the spheroid formation: 20,000 cells/drop for the endometrial stromal cell lines ST-T1b, tHESC, and D-tHESC,

and 2000 cells/drop for trophoblast cells JEG3 and HTR8/SVneo. The spheroids were monitored to assess morphology and compactness using inverted microscopy under 10× magnification (Leica microsystems, Wetzlar, Germany). Spheroid diameter measurements were obtained from independent biological replicates. Within each replicate, all generated spheroids were included in the analysis, and the reported sample sizes represent the total number of spheroids pooled across replicates. Diameters of individual spheroids were quantified using ImageJ 1.54g as well as with Leica Application Suite V4.8.

#### 2.4. Freezing and Thawing of Spheroids

The spheroids formed were frozen for future applications in a medium consisting of the respective culture medium based on the cell type (80%), FBS (10%), and dimethyl sulfoxide (DMSO, 10%). Approximately 10 spheroids were collected per 1.5 mL Eppendorf tube, suspended in 1 mL of freezing medium, and stored at  $-80^{\circ}\text{C}$  for further use. For thawing, the tubes with frozen spheroids were placed in a water bath ( $\sim 37^{\circ}\text{C}$ ) for 2 min. Once thawed completely, supernatant was removed and spheroids were collected using a pipette tip and placed as a drop on the lid of a culture dish. In total, 50  $\mu\text{L}$  PBS was used for washing the spheroid to remove the residual freezing medium before proceeding with the post-thaw morphology and viability assessment.

#### 2.5. Viability of Frozen Spheroids

The thawed and washed spheroids were tested for their viability with the Calcein-AM staining [27]. The spheroids were then transferred into 96-well microplates (Thermo Scientific™, Rheinfelden, Germany), with each well containing 50  $\mu\text{L}$  of PBS to prevent dehydration. For the viability assessment, 1  $\mu\text{L}$  Calcein-AM stock solution (4 mM diluted in 100 mL DMSO, Millipore GmbH, Rockville-MD, USA) was diluted further in 1 mL DPBS. A total of 100  $\mu\text{L}$  of this prepared staining solution was added to each well. The plate was then incubated at  $37^{\circ}\text{C}$  for 30 min. Following incubation, spheroids were visualized using inverted green fluorescence microscopy (Leica microsystems, Wetzlar, Germany) with a fluorescein isothiocyanate (FITC) filter, (excitation 480/40 nm, emission 527/30 nm, Leica microsystems) under 10× magnification indicating the viability of the spheroids.

### 3. Results

#### 3.1. Validation of Spheroid Formation Using Different Cell Lines

In order to establish reproducible 3D culture conditions, we initially optimized the spheroid formation by testing key parameters such as cell concentration and the impact of MC using cell lines widely studied in reproduction: tHESC (both decidualized and non-decidualized) and the trophoblast-derived JEG3 cells, using the hanging drop method. Spheroid formation was investigated under different cell concentrations and with/without MC ( $n = 5$ ). The MC significantly promoted the formation and the maintenance of the integrity of the 3D structure in both cell types and in both cell concentrations (Figure 1). In the higher cell concentration (20,000 cells/drop) with MC (Figure 1A,E,I), all cell lines (JEG-3, tHESC and D-tHESC) formed large and cohesive spheroids with smooth and well-defined edges, whereas without MC (Figure 1B,F,J), all cell lines formed loose aggregates or monolayer-like clusters. A comparable pattern was observed in all cell lines at the lower cell concentration (2000 cells/drop); with MC (Figure 1C,G,K), smaller yet well-structured spheroids were formed, whereas in the absence of MC (Figure 1D,H,L), non-spherical aggregates were observed.

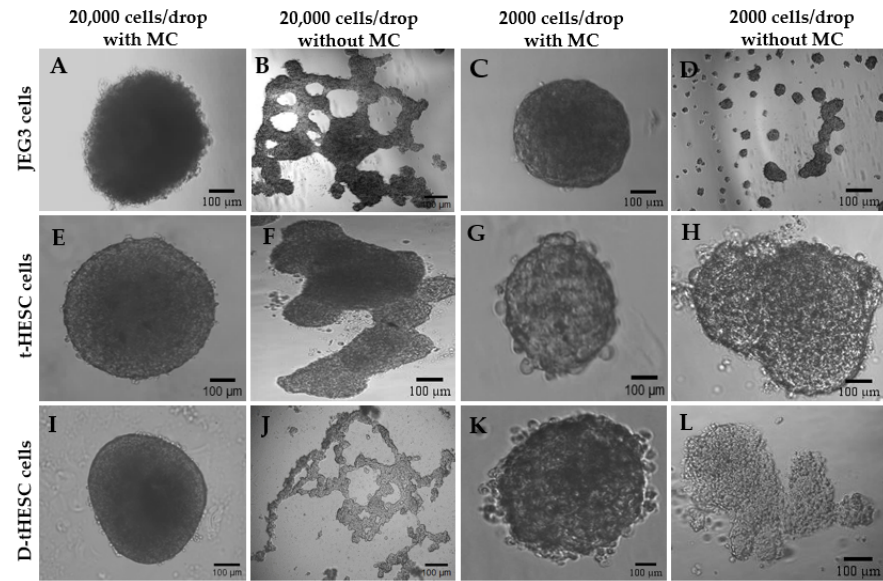


**Figure 1.** Validation of spheroid formation by JEG3, tHESC, and D-tHESC under varying conditions of cell concentration and with and without MC, observed using inverted microscopy (10 $\times$ ). (A) JEG3, 20,000 cells/drop with MC; (B) JEG3, 20,000 cells/drop without MC; (C) JEG3, 2000 cells/drop with MC; (D) JEG3, 2000 cells/drop without MC; (E) tHESC, 20,000 cells/drop with MC; (F) tHESC, 20,000 cells/drop without MC; (G) tHESC, 2000 cells/drop with MC; (H) tHESC, 2000 cells/drop without MC; (I) D-tHESC, 20,000 cells/drop with MC; (J) D-tHESC, 20,000 cells/drop without MC; (K) D-tHESC, 2000 cells/drop with MC; (L) D-tHESC, 2000 cells/drop without MC.

Based on the reproducible results ( $n = 25$  spheroids), conditions with MC were the most effective regardless of the cell concentration tested. The trophoblast cells were highly proliferative and loosely cohesive. Therefore, it was decided to consider lower cell concentrations for JEG3 (Figure 1) (2000 cells/drop) to ensure structural integrity and to prevent overcrowding. In contrast, stromal cells (decidualized and non-decidualized) (Figure 1) only formed stable spheroids at higher concentrations (20,000 cells/drop). To evaluate the transferability, the discovered optimized conditions were tested with the additional cell lines (Figure 2), StT1b (endometrial) and HTR8/SVneo (trophoblast).

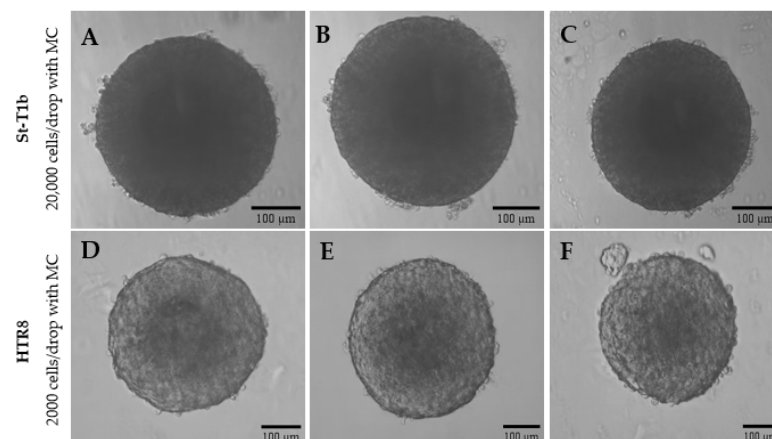


**Figure 2.** Spheroid formation of St-T1b and HTR8/SVneo cell lines under optimized conditions, visualized under inverted microscopy (10 $\times$ ). (A–C) St-T1b, 20,000 cells/drop with MC; (D–F) HTR8/SVneo, 2000 cells/drop with MC.

The diameter data of all cell lines are presented as a descriptive analysis to illustrate spheroid size variability across experiments. D-tHESC spheroids with a cell concentration of 20,000 cells/drop with MC revealed an average diameter of  $530 \pm 80.81 \mu\text{m}$  ( $n = 30$ ).

Similarly, spheroids from tHESC and St-T1b (20,000 cells/drop) with MC had an average diameter of  $572.42 \pm 77.09 \mu\text{m}$  ( $n = 50$ ), and  $558.99 \pm 52.80 \mu\text{m}$  ( $n = 52$ ), respectively. The diameters of the trophoblast spheroids with the cell concentration of 2000 cells/drop with MC were  $324.39 \pm 24.63 \mu\text{m}$  ( $n = 50$ ) for HTR8/SVneo cells, and  $338.46 \pm 30.25 \mu\text{m}$  ( $n = 50$ ) for JEG-3 cells.

The experiments showed that both the cell lines St-T1b (20,000 cell/drop with MC) and HTR8/SVneo (2000 cells/drop with MC) (Figure 2) formed compact, well-defined, and uniform spheroids similar to tHESC and JEG3 spheroids under the established conditions. Spheroid formation was observed in all seeded drops (100% efficiency) under the optimized conditions, irrespective of the cell type tested (tHESC, JEG3, St-T1b, and HTR8/SVneo).

A temporal dynamics study was applied across all cell lines (Figure 3A,B). At the time point 0 h, the cells were dispersed within the hanging drop, followed by the formation of aggregates in all cell lines by 8 h. The aggregation of HTR8/SVneo cells was less pronounced compared to the other cell lines. By 24 h, aggregated cells began to compact. However, spheroids of St-T1b, t-HESC, and D-tHESC cells still appeared irregular and distorted in shape, whereas JEG3 spheroids looked crowded, and HTR8/SVneo cells showed tightly packed structures. By 32 h, the spheroids of the different cell lines, except D-tHESC, achieved a rounded and well-defined morphology, which stabilized further into compact spheroids by 48 h (Figure 3A). D-tHESC required a longer culture period and reached a compact morphology by 72 h (Figure 3B).

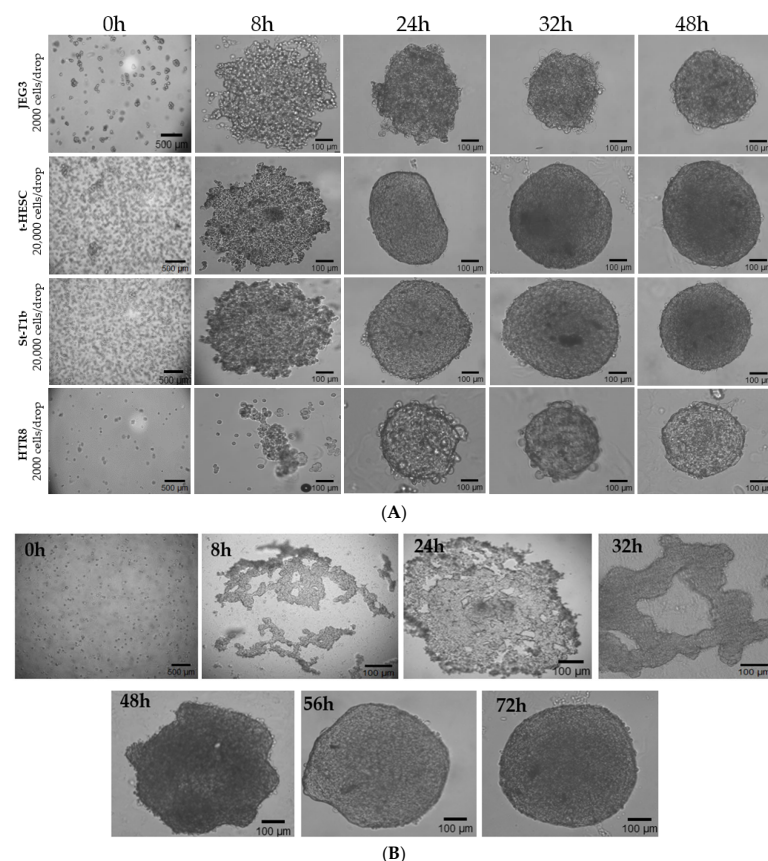


**Figure 3.** (A) Temporal analysis of spheroid formation of trophoblast and ES cell lines. Spheroids formed using the hanging drop model at different time points (0 h, 8 h, 24 h, 32 h, and 48 h) observed in inversion microscopy under  $4\times$  (0 h) and  $10\times$  (8–48 h). (B) Time-dependent analysis of spheroid formation of D-tHESC cells (20,000 cells/drop) using the hanging drop model. Inverted microscope magnification of  $4\times$  (0 h) and  $10\times$  (8–72 h).

### 3.2. Freezing of Spheroids

Spheroids of all tested cell lines (non-decidualized tHESC, JEG3, St-T1b, and HTR8/SVneo) were frozen using conventional freezing medium. They stayed frozen for 11 months to determine whether their viability and morphology could be maintained. The thawing process was performed as mentioned above (see Section 2.5) and spheroids were examined for viability and structural integrity. Furthermore, extended observations indicated that these spheroids maintained functional viability for up to 72 h post-thaw.

Spheroids from all cell lines ( $n = 20$  spheroids per cell line) were evaluated after thawing using inverted microscopy (Figure 4). Furthermore, Calcein-AM staining analyzed by inverted microscopy (Figure 5) revealed a high post-thaw viability of spheroids.

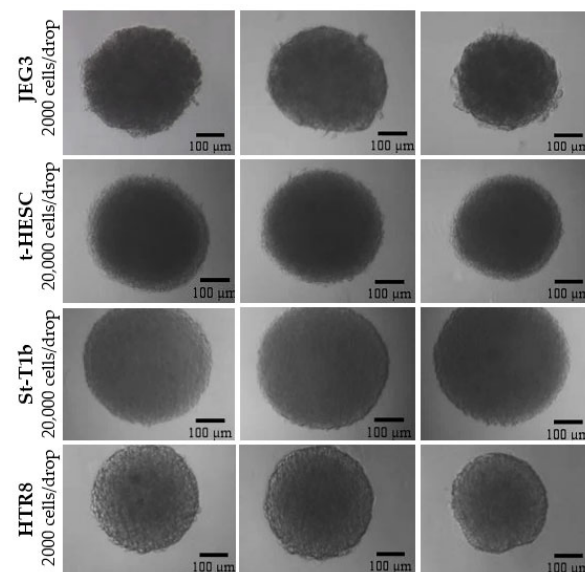


**Figure 4.** Morphology of spheroids from different cell lines (tHESC, St-T1b, JEG3, and HTR8/SVneo) immediately after thawing, observed under inverted microscopy (10 $\times$ ).

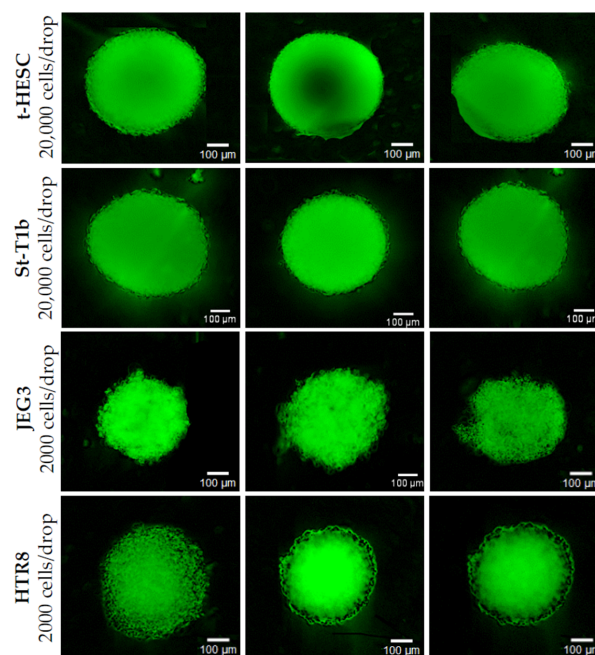


**Figure 5.** Viability assessment of spheroids using Calcein staining observed under inverted green fluorescence microscopy (10 $\times$ ).

#### 4. Discussion

In this study, we validated and established an optimized protocol for spheroid formation using the hanging drop model with commonly used cell lines in the field of reproductive biology. For this, two endometrial cell lines: tHESC (decidualized and un-decidualized) and St-T1b; and two trophoblast cell lines: HTR8/SVneo and JEG3 were analyzed with regard to establishing the optimal culture conditions for spheroid formation on the one hand, and to the freezing of spheroids enabling long-term storage and maintaining viability on the other hand.

The supplementation of MC in the culture system markedly improved the formation of stable and well-defined spheroids which was observed in all biological replicates of all four different cell lines. This is consistent with previous research emphasizing that MC, an inert and biocompatible additive, enhances cell aggregation and spheroid formation by increasing the viscosity of the culture medium and thereby supporting the stable 3D structures [27]. This additive reduces the mono-layering of cells and so supports the formation of uniform, tightly packed spheroids, essential for reproducible and physiologically relevant 3D models. We have optimized the cell concentration for each cell type based on its proliferation characteristics. The stromal cell line tHESC exhibited a modest proliferation rate and stronger adhesive properties, forming tightly packed spheroids at higher cell concentrations (20,000 cells/drop). In contrast, the highly progressive trophoblast cells formed compact spheroids at lower concentrations (2000 cells/drop) [28,29]. These conditions, which were optimized with tHESC and JEG3 cells, were subsequently applied to the St-T1b and HTR8/SVneo cell lines. The temporal analysis showed that spheroid formation began within 8 h of seeding. Over the next 24 h, these cell aggregates progressively compacted into a well-structured spheroid, reaching its morphological stability by 48 h. It was demonstrated that the presence of MC played a crucial role in facilitating faster aggregation and maintaining the integrity of the spheroids. Spheroid formation is observed in all seeded drops for all cell lines, corresponding to a 100% formation efficiency under optimized conditions. In comparison, a previous study [30] reported ~100% efficiency for HTR8/SVneo cells but only ~50% efficiency for JEG3 cells using the inverted hanging drop system. These differences likely reflect variations in seeding density, methyl cellulose supplementation, and culture conditions. Our optimized protocol produces structurally stable and reproducible spheroids suitable for downstream assays. Notably, HTR8/SVneo cells were easier to handle than JEG3 cells, consistent with general observations of their aggregation behavior. To place the optimized hanging drop methyl cellulose approach in the broader context of currently available 3D spheroid culture systems, we compared key methodological and practical aspects of our model with other commonly used spheroid formation platforms, as summarized in Table 1.

**Table 1.** Comparison of spheroid formation methods. This table compares our hanging drop method with methyl cellulose (MC) and commonly used 3D spheroid formation approaches across key features such as cost, uniformity, ease of setup, scaffold requirement, scalability, and monitoring.

Feature/ Aspect	Our Study—Hanging Drop Model with Methyl Cellulose (MC)	Existing 3D Spheroid Formation Approaches
Cost	Low—The hanging drop method requires minimal equipment and commonly available reagents, making it cost-effective [31].	Variable—Methods such as spinner flasks, microfluidic platforms, and automated systems often require specialized equipment and higher initial investment [32].
Uniformity of spheroid size	High—Spheroid size and compactness can be effectively controlled by optimizing cell density and with MC.	Ultra-low attachment plates may show difficulty in forming compact spheroids for certain cell lines; spinner flasks, rotating wall vessels, and micropatterned plates can result in size heterogeneity unless conditions are carefully optimized [33].

Table 1. Cont.

Feature/Aspect	Our Study—Hanging Drop Model with Methyl Cellulose (MC)	Existing 3D Spheroid Formation Approaches
Ease of setup/simplicity	Simple workflow—Easy to establish without specialized devices or complex procedures.	Some approaches, including microfluidic systems and bioreactors, require complex fabrication, assembly, or operational expertise [32].
Requirement for matrix/scaffold	Spheroid formation is achieved under scaffold-free conditions using the hanging drop method. Methyl cellulose is used solely as a viscosity-enhancing supportive additive to promote cell aggregation and spheroid stability, without providing extracellular matrix or structural support.	Several widely used 3D culture methods rely on solid scaffolds or ECM-based matrices, including Matrigel-embedded cultures, collagen or fibrin hydrogels, alginate- or PEG-based hydrogels, and ECM-coated microcarrier systems, which provide physical structure and biochemical cues that may influence cell behavior [34].
Scalability	Moderate—Suitable for generating small to medium numbers of spheroids; manual handling limits large-scale production [31].	Automated or high-throughput platforms such as ultra-low attachment plates and spinner flasks enable large-scale spheroid production and higher throughput [33].
Monitoring/real-time observation	Easy—Spheroid formation and morphological changes can be directly monitored in hanging drops using standard light microscopy without disturbing the culture.	Scaffold-based or matrix-embedded systems can limit direct optical observation due to matrix density and diffusion constraints, often requiring specialized imaging approaches (e.g., confocal or light-sheet microscopy) or endpoint analyses [35].
Medium exchange/experimental manipulation	Medium exchange is more challenging; the small droplet volume requires careful handling and may disrupt spheroid integrity [36].	Ultra-low attachment plates and well-based systems facilitate easier medium exchange, compound addition, and repeated treatments [33].

Decidualization plays a major role in successful implantation and pregnancy maintenance. *In vitro* decidualization of human endometrial stromal cells is commonly validated by prolactin secretion, which represents a robust functional marker of decidual differentiation. Although IGFBP-1 is frequently assessed in parallel, several recent studies have demonstrated that quantification of prolactin alone is sufficient to confirm decidualization in hormone-stimulated stromal cultures [37–39]. Therefore, under the controlled experimental conditions used in this study, prolactin secretion was considered an appropriate and accepted marker of decidualization. It changes the morphology and functionality of ES cells including reduced proliferation and enhanced adhesive properties [40]. Notably, this is the first report demonstrating successful generation of spheroids from D-tHESCs. Compared to non-decidualized tHESCs, D-tHESCs exhibited stronger cell–cell adhesion and enhanced extracellular matrix production, which limited complete dissociation and influenced aggregation dynamics. These decidualization-associated phenotypic changes likely contributed to the extended spheroid formation period, with D-tHESCs requiring 72 h to form compact spheroids compared to 48 h for non-decidualized cells. The establishment of D-tHESC spheroids offers a novel and highly needed platform to study decidual remodeling and embryo–maternal communication.

Spheroid formation progresses through different stages such as cell aggregation, compaction, and growth [41], with morphology and temporal differences driven by specific cell adhesion properties and cytoskeletal dynamics. Using the hanging drop model, all cell types investigated in this study aggregated within 8 h; however, their kinetics of compaction and stabilization varied. HTR8/SVneo trophoblast cells displayed less aggregation compared to JEG3, which aligns with a previous study mentioning that HTR8/SVneo form stable and compact spheroids, whereas JEG3 cells often form irregular and loose aggregates [30]. Even though the spheroids of D-tHESC, tHESC and St-T1b showed undefined structures at 24 h, they gradually developed to a very well-defined and compact structure

by 48 h for tHESC and St-T1b and 72 h for D-tHESC. This delayed compaction is consistent with previous observations in stromal spheroid models where extracellular matrix (ECM) remodeling occurs more slowly and is associated with coordinated collagen reorganization [42]. Trophoblast and epithelial-like cell lines typically form spheroids faster compared to stromal cell lines because the cells have stronger cadherin-mediated adhesion and more robust cytoskeletal contractility, resulting in rapid aggregation and compaction [19]. This variability in compaction efficiencies across different cell types is well known and reflects intrinsic differences in adhesion strength, contractility, and ECM interaction profiles [43]. Based on our observations, we speculate that the 72 h spheroid formation in D-tHESCs versus 48 h in non-decidualized t-HESCs is due to the shift toward ECM remodeling associated with decidualization [44], along with decreased actomyosin contractility and altered integrin/cadherin expression [45]. Additionally, compared to non-decidualized stromal cells, decidual cells modify their pericellular matrix and reorganize collagens I, III, IV and VI more extensively which may further contribute to slower spheroid formation [46]. Furthermore, decidualization has been reported to reduce Rho/ROCK signaling and stromal cell contractility, resulting in mechanically softer cytoskeletons that could potentially slow the compaction of spheroids [47]. Collectively, these considerations support our hypothesis that variations in ECM remodeling kinetics, cytoskeletal tension, and cell–cell adhesion may contribute to the slower temporal dynamics of D-tHESC spheroid formation. It emphasizes the importance of defining cell type-specific culture durations for spheroid formation to avoid any misinterpretation in functional assays.

Studies regarding freezing/thawing of spheroids from reproductive tissue cell lines remain limited. As the application of 3D models in reproductive research is in high demand to elucidate and mimic the *in vivo* environment, establishing reliable storage methods for these structures is essential. Our study highlights the protocol of long-term storage of 3D spheroids using a standard conventional freezing medium and storage at  $-80^{\circ}\text{C}$ . This method was tested across four different cell lines. The frozen spheroids thawed after 11 months of storage retained their viability and structural integrity. A previous study reported a cryopreservation protocol [48] on mesenchymal stromal cell spheroids which involved procedures using controlled-rate freezing and storage in liquid nitrogen ( $-196^{\circ}\text{C}$ ) or at  $-80^{\circ}\text{C}$  followed by immersion in liquid nitrogen, whereas our approach provides a simpler and more flexible freezing method that supports flexibility in the experimental setup. Similarly, another study [49] on mesenchymal stromal cell spheroids stated that freezing with DMSO and 5% FBS maintained stemness and viability; however, they only tested storage after 1 week. Our results extend these findings by showing that spheroids remain viable and functional even after longer storage periods of several months.

Moreover, it is suggested in a few articles that extracellular cryoprotectants such as trehalose, starch derivative or serum proteins play a major role in maintaining post-thaw viability especially in tumor spheroids stored in a culture medium along with cryoprotective agents [15]. Another study investigated alternative cryoprotective formulations by introducing carbohydrate-based macromolecular crowders like Polydextrose III, alternative to FBS which exhibited consistent post-thaw results such as structural stability and viability [16]. However, our standard and simple freezing method offers comparable post-thaw results and proved effective for our reproductive cell models.

Our findings emphasize that a standard and conventional freezing method provides a simple and reproducible way to store spheroids in the long term. Spheroids frozen up to 11 months maintained sufficient viability for experimental applications. This validates the robustness of the freezing method allowing very flexible experimental planning, while facilitating downstream functional assays and minimizing the need for frequent spheroid formation. This finding could support their use in long-term studies and reproducible

experiments. It depicts that the spheroid structure remained intact, with minimal disruption to their 3D structure.

Importantly, our optimized spheroid model provides a physiologically relevant 3D platform for studying early pregnancy processes, including embryo–endometrial interactions [3], trophoblast adhesion [50], invasion, and paracrine signaling [51]. By better mimicking *in vivo* cell–cell and microenvironment interactions than conventional 2D cultures [52], these spheroids enable more meaningful functional and mechanistic studies. Additionally, the demonstrated feasibility of long-term freezing enhances experimental reproducibility, making this model adaptable for downstream applications in reproductive biology.

## 5. Conclusions

Spheroid formation was systematically optimized for various stromal and trophoblast cell lines by testing key parameters such as cell concentration and MC supplementation. The resulting spheroids exhibited well-defined morphology, structural integrity, and viability, thus enabling their use for downstream applications. Furthermore, an approach to freeze and store spheroids in the long-term using the conventional medium was established, showing a well-maintained viability and cellular architecture of post-thaw spheroids. This work provides a baseline foundation for forming and preserving spheroids without substantial loss of functionality. Beyond the application in the scope of trophoblast–stromal research, the principle outlined here can be adapted for other 3D multicellular models in broader fields, e.g., in toxicology, developmental biology, and translational research. Future work will include these optimized spheroids into dynamic co-culture and confrontation models for invasion and response treatment studies and paves a pathway for more physiologically relevant, flexible, and reproductive models in reproductive research.

## 6. Reagents Setup

The prepared methyl cellulose stock solution can be stored for up to 3 months at 4 °C.

**Supplementary Materials:** The following supporting information can be downloaded at: <https://www.mdpi.com/article/10.3390/mps9010027/s1>, Figure S1: Representation of prolactin secretion by tHESC cells as evidence of decidualization; Figure S2: Microscopic observation of D-tHESC during experimentation with cell concentration and methyl cellulose supplementation across replicates; Figure S3: Microscopic observation of tHESC during experimentation with cell concentration and methyl cellulose supplementation across replicates; Figure S4: Microscopic observation of JEG3 during experimentation with cell concentration and methyl cellulose supplementation across replicates; Figure S5: Microscopic observation of D-tHESC with 20,000 cells/drop with methyl cellulose across replicates; Figure S6: Microscopic observation of tHESC with 20,000 cells/drop with methyl cellulose across replicates; Figure S7: Microscopic observation of St-T1b with 20,000 cells/drop with methyl cellulose across replicates; Figure S8: Microscopic observation of JEG3 with 2000 cells/drop with methyl cellulose across replicates; Figure S9: Microscopic observation of HTR8 with 2000 cells/drop with methyl cellulose across replicates; Figure S10: Representation of Calcein-AM staining on frozen spheroids from different cell lines to assess viability; Table S1: Dataset including individual spheroid diameter measurements along with mean and standard deviation values for each cell line.

**Author Contributions:** Conceptualization and experimental design, A.P.B. and D.M.B.-B.; collected the data and contributed to analysis, K.M., I.S., A.P.B. and D.M.B.-B.; performed the analysis, K.M., I.S. and J.B.-L.; wrote the paper, K.M., I.S., D.M.B.-B., J.B.-L. and A.P.B.; edited the paper, A.P.B., J.-S.K., D.M.B.-B., I.S. and K.M.; administered the project, A.P.B. and D.M.B.-B.; acquired the funding, A.P.B. All authors have read and agreed to the published version of the manuscript.

**Funding:** This research was supported by the Deutsche Forschungsgemeinschaft (DFG, BI1963/11-1; project number—537607142).

**Institutional Review Board Statement:** Not applicable; the source of the cell line has been stated in the Materials and Methods Section.

**Informed Consent Statement:** Not applicable.

**Data Availability Statement:** The original contributions presented in this study are included in the article/Supplementary Material. Further inquiries can be directed to the corresponding author.

**Acknowledgments:** I would like to thank Udo R. Markert, Frauke von Versen-Höynck and Ruth Grümmer for their valuable support in discussing my results. I am also grateful for their insightful suggestions and guidance throughout this work. Finally, I would like to acknowledge the encouragement and assistance of my colleagues and lab members during the research.

**Conflicts of Interest:** The authors declare no conflicts of interest.

## Abbreviations

The following abbreviations are used in this manuscript:

3D	Three-dimensional
MC	Methyl cellulose
ES	Endometrial stromal
D-tHESC	Decidualized tHESC
DMEM	Dulbecco's Modified Eagle Medium
FBS	Fetal bovine serum
P/S	Penicillin-streptomycin
PBS	Phosphate-buffered saline
DMSO	Dimethyl sulfoxide
FITC	Fluorescein isothiocyanate
ECM	Extracellular matrix

## References

1. Wanigasekara, J.; Carroll, L.J.; Cullen, P.J.; Tiwari, B.; Curtin, J.F. Three-Dimensional (3D) in vitro cell culture protocols to enhance glioblastoma research. *PLoS ONE* **2023**, *18*, e0276248. [[CrossRef](#)] [[PubMed](#)]
2. Lee, N.H.; Bayaraa, O.; Zechu, Z.; Kim, H.S. Biomaterials-assisted spheroid engineering for regenerative therapy. *BMB Rep.* **2021**, *54*, 356–367. [[CrossRef](#)] [[PubMed](#)]
3. Li, X.; Kodithuwakku, S.P.; Chan, R.W.; Yeung, W.S.; Yao, Y.; Ng, E.H.Y.; Chiu, P.C.; Lee, C.L. Three-dimensional culture models of human endometrium for studying trophoblast-endometrium interaction during implantation. *Reprod. Biol. Endocrinol.* **2022**, *20*, 120. [[CrossRef](#)] [[PubMed](#)]
4. Arora, S.; Singh, S.; Mittal, A.; Desai, N.; Khatri, D.K.; Gugulothu, D.; Lather, V.; Pandita, D.; Vora, L.K. Spheroids in cancer research: Recent advances and opportunities. *J. Drug Deliv. Sci. Technol.* **2024**, *100*, 106033. [[CrossRef](#)]
5. Shao, C.; Chi, J.; Zhang, H.; Fan, Q.; Zhao, Y.; Ye, F. Development of Cell Spheroids by Advanced Technologies. *Adv. Mater. Technol.* **2020**, *5*, 2000183. [[CrossRef](#)]
6. Hattermann, K.; Held-Feindt, J.; Mentlein, R. Spheroid confrontation assay: A simple method to monitor the three-dimensional migration of different cell types in vitro. *Ann. Anat.-Anat. Anz.* **2011**, *193*, 181–184. [[CrossRef](#)]
7. Maritan, S.M.; Lian, E.Y.; Mulligan, L.M. An Efficient and Flexible Cell Aggregation Method for 3D Spheroid Production. *J. Vis. Exp.* **2017**, *121*, 55544.
8. Li, R.; Wang, T.Y.; Shelp-Peck, E.; Wu, S.P.; DeMayo, F.J. The single-cell atlas of cultured human endometrial stromal cells. *FS Sci.* **2022**, *3*, 349–366. [[CrossRef](#)]
9. Samalecos, A.; Reimann, K.; Wittmann, S.; Schulte, H.M.; Brosens, J.J.; Bamberger, A.M.; Gellersen, B. Characterization of a novel telomerase-immortalized human endometrial stromal cell line, St-T1b. *Reprod. Biol. Endocrinol.* **2009**, *7*, 76. [[CrossRef](#)]
10. Abbas, Y.; Turco, M.Y.; Burton, G.J.; Moffett, A. Investigation of human trophoblast invasion in vitro. *Hum. Reprod. Update* **2020**, *26*, 501–513. [[CrossRef](#)]

11. Grümmer, R.; Hohn, H.P.; Denker, H.W. Choriocarcinoma Cell Spheroids: An In Vitro Model for the Human Trophoblast. In *Trophoblast Invasion and Endometrial Receptivity: Novel Aspects of the Cell Biology of Embryo Implantation*; Denker, H.-W., Aplin, J.D., Eds.; Springer: Boston, MA, USA, 1990; pp. 97–111.
12. Grümmer, R.; Hohn, H.P.; Mareel, M.M.; Denker, H.W. Adhesion and invasion of three human choriocarcinoma cell lines into human endometrium in a three-dimensional organ culture system. *Placenta* **1994**, *15*, 411–429. [[CrossRef](#)]
13. Buck, V.U.; Flensburg, F.; Krings, O.; Leube, R.E.; Gellersen, B.; Classen-Linke, I. Trophoblast-Endometrial Interaction in a 3D Culture System. *Placenta* **2013**, *34*, A31. [[CrossRef](#)]
14. Marquez-Curtis, L.A.; Janowska-Wieczorek, A.; McGann, L.E.; Elliott, J.A.W. Mesenchymal stromal cells derived from various tissues: Biological, clinical and cryopreservation aspects. *Cryobiology* **2015**, *71*, 181–197. [[CrossRef](#)] [[PubMed](#)]
15. Ehrhart, F.; Schulz, J.C.; Katsen-Globa, A.; Shirley, S.G.; Reuter, D.; Bach, F.; Zimmermann, U.Z.; Zimmermann, H. A comparative study of freezing single cells and spheroids: Towards a new model system for optimizing freezing protocols for cryobanking of human tumours. *Cryobiology* **2009**, *58*, 119–127. [[CrossRef](#)] [[PubMed](#)]
16. Hans, A.; Salil Sawant, P.; Ajaonkar, B.; Jain, R.; Dandekar, P. Cryopreservation of human lung adenocarcinoma spheroids using MMC based cryomixtures. *J. Biomater. Sci. Polym. Ed.* **2025**, *36*, 2311–2332. [[CrossRef](#)]
17. Park, J.J.; Lee, O.-H.; Park, J.-E.; Cho, J. Comparison of Cryopreservation Media for Mesenchymal Stem Cell Spheroids. *Biopreserv. Biobank.* **2023**, *22*, 486–496. [[CrossRef](#)]
18. Okada, H.; Tsuzuki, T.; Murata, H. Decidualization of the human endometrium. *Reprod. Med. Biol.* **2018**, *17*, 220–227. [[CrossRef](#)]
19. Gellersen, B.; Brosens, J.J. Cyclic decidualization of the human endometrium in reproductive health and failure. *Endocr. Rev.* **2014**, *35*, 851–905. [[CrossRef](#)]
20. Gellersen, B.; Brosens, I.A.; Brosens, J.J. Decidualization of the human endometrium: Mechanisms, functions, and clinical perspectives. *Semin. Reprod. Med.* **2007**, *25*, 445–453. [[CrossRef](#)]
21. Gonzalez, M.; Neufeld, J.; Reimann, K.; Wittmann, S.; Samalecos, A.; Wolf, A.; Bamberger, A.-M.; Gellersen, B. Expansion of human trophoblastic spheroids is promoted by decidualized endometrial stromal cells and enhanced by heparin-binding epidermal growth factor-like growth factor and interleukin-1  $\beta$ . *Mol. Hum. Reprod.* **2011**, *17*, 421–433. [[CrossRef](#)]
22. Brosens, J.J.; Takeda, S.; Acevedo, C.H.; Lewis, M.P.; Kirby, P.L.; Symes, E.K.; Krausz, T.; Purohit, A.; Gellersen, B.; White, J.O. Human endometrial fibroblasts immortalized by simian virus 40 large T antigen differentiate in response to a decidualization stimulus. *Endocrinology* **1996**, *137*, 2225–2231. [[CrossRef](#)] [[PubMed](#)]
23. Kohler, P.O.; Bridson, W.E. Isolation of hormone-producing clonal lines of human choriocarcinoma. *J. Clin. Endocrinol. Metab.* **1971**, *32*, 683–687. [[CrossRef](#)] [[PubMed](#)]
24. Graham, C.H.; Hawley, T.S.; Hawley, R.C.; MacDougall, J.R.; Kerbel, R.S.; Khoo, N.; Lala, P.K. Establishment and Characterization of First Trimester Human Trophoblast Cells with Extended Lifespan. *Exp. Cell Res.* **1993**, *206*, 204–211. [[CrossRef](#)] [[PubMed](#)]
25. Scheliga, I.A.-O.; Baston-Buest, D.A.-O.; Haramustek, D.; Knebel, A.; Kruessel, J.A.-O.; Bielfeld, A.A.-O. Dead or Alive: Exploratory Analysis of Selected Apoptosis- and Autophagy-Related Proteins in Human Endometrial Stromal Cells of Fertile Females and Their Potential Role During Embryo Implantation. *Int. J. Mol. Sci.* **2025**, *26*, 175. [[CrossRef](#)]
26. Tetzlaff, F.; Fischer, A. Human Endothelial Cell Spheroid-based Sprouting Angiogenesis Assay in Collagen. *Bio-Protoc.* **2018**, *8*, e2995. [[CrossRef](#)]
27. Sanfilippo, S.; Canis, M.; Ouchchane, L.; Botchorishvili, R.; Artonne, C.; Janny, L.; Brugnon, F. Viability assessment of fresh and frozen/thawed isolated human follicles: Reliability of two methods (Trypan blue and Calcein AM/ethidium homodimer-1). *J. Assist. Reprod. Genet.* **2011**, *28*, 1151–1156. [[CrossRef](#)]
28. Leung, B.M.; Leshner-Perez, S.C.; Matsuoka, T.; Moraes, C.; Takayama, S. Media additives to promote spheroid circularity and compactness in hanging drop platform. *Biomater. Sci.* **2015**, *3*, 336–344. [[CrossRef](#)]
29. Schellino, R.; Boido, M.; Vercelli, A. JNK Signaling Pathway Involvement in Spinal Cord Neuron Development and Death. *Cells* **2019**, *8*, 1576. [[CrossRef](#)]
30. Weber, M.; Knoefler, I.; Schleussner, E.; Markert, U.R.; Fitzgerald, J.S. HTR8/SVneo cells display trophoblast progenitor cell-like characteristics indicative of self-renewal, repopulation activity, and expression of "stemness"- associated transcription factors. *BioMed Res. Int.* **2013**, *2013*, 243649. [[CrossRef](#)]
31. Lonkwic, K.M.; Zajdel, R.; Kaczka, K. Unlocking the Potential of Spheroids in Personalized Medicine: Systematic Review of Seeding Methodologies. *Int. J. Mol. Sci.* **2025**, *26*, 6478. [[CrossRef](#)]
32. Velasco, V.; Shariati, S.A.; Esfandyarpour, R. Microtechnology-based methods for organoid models. *Microsyst. Nanoeng.* **2020**, *6*, 76. [[CrossRef](#)] [[PubMed](#)]
33. Pinto, B.; Henriques, A.C.; Silva, P.M.A.; Bousbaa, H. Three-Dimensional Spheroids as In Vitro Preclinical Models for Cancer Research. *Pharmaceutics* **2020**, *12*, 1186. [[CrossRef](#)] [[PubMed](#)]
34. Lopez-Vince, E.; Simon-Yarza, T.; Wilhelm, C. A polysaccharide-based hydrogel platform for tumor spheroid production and anticancer drug screening. *Sci. Rep.* **2025**, *15*, 4213. [[CrossRef](#)] [[PubMed](#)]

35. Temple, J.; Velliou, E.; Shehata, M.; Lévy, R.; Gupta, P. Current strategies with implementation of three-dimensional cell culture: The challenge of quantification. *Interface Focus* **2022**, *12*, 20220019. [[CrossRef](#)]
36. Cha, Y.S.; Michaels, A.; Wang, J.Z.; Niu, Y.; Lin, Y.; Zhu, L.; Zhu, X.; Wang, K.; Murray, M.; Zhou, F. Recent advances in 3D cell culture models in cancer drug development. *J. Pharm. Investig.* **2025**, *55*, 557–573. [[CrossRef](#)]
37. Tanaka, S.; Sawachika, M.; Yoshida, N.; Futani, K.; Murata, H.; Okada, H. IL17A Suppresses IGFBP1 in Human Endometrial Stromal Cells. *Reprod. Med.* **2024**, *5*, 43–56. [[CrossRef](#)]
38. Platt, F.; Moyer, J.; Singer, B.B.; Baston-Büst, D.; Wennemuth, G.; Bielfeld, A.P.; Grümmer, R. Forskolin versus cAMP-Induced Decidualization and Survival of Endometrial Stromal Cells of Endometriosis Patients. *Reprod. Sci.* **2023**, *30*, 2680–2691. [[CrossRef](#)]
39. Zambuto, S.G.; Theriault, H.; Jain, I.; Crosby, C.O.; Pintescu, I.; Chiou, N.; Oyen, M.L.; Zoldan, J.; Underhill, G.H.; Harley, B.A.C.; et al. Endometrial decidualization status modulates endometrial microvascular complexity and trophoblast outgrowth in gelatin methacryloyl hydrogels. *npj Womens Health* **2024**, *2*, 22. [[CrossRef](#)]
40. Cook, C.D.; Hill, A.S.; Guo, M.; Stockdale, L.; Papps, J.P.; Isaacson, K.B.; Lauffenburger, D.A.; Griffith, L.G. Local remodeling of synthetic extracellular matrix microenvironments by co-cultured endometrial epithelial and stromal cells enables long-term dynamic physiological function. *Integr. Biol.* **2017**, *9*, 271–289. [[CrossRef](#)]
41. Smyrek, I.; Mathew, B.; Fischer, S.C.; Lissek, S.M.; Becker, S.; Stelzer, E.H.K. E-cadherin, actin, microtubules and FAK dominate different spheroid formation phases and important elements of tissue integrity. *Biol. Open* **2019**, *8*, bio037051. [[CrossRef](#)]
42. Stejskalová, A.; Fincke, V.; Nowak, M.; Schmidt, Y.; Borrmann, K.; von Wahlde, M.-K.; Schäfer, S.D.; Kiesel, L.; Greve, B.; Götte, M. Collagen I triggers directional migration, invasion and matrix remodeling of stroma cells in a 3D spheroid model of endometriosis. *Sci. Rep.* **2021**, *11*, 4115. [[CrossRef](#)] [[PubMed](#)]
43. Han, S.J.; Kwon, S.; Kim, K.S. Challenges of applying multicellular tumor spheroids in preclinical phase. *Cancer Cell Int.* **2021**, *21*, 152. [[CrossRef](#)] [[PubMed](#)]
44. Favaro, R.; Abrahamsohn, P.A.; Zorn, M.T. 11-Decidualization and Endometrial Extracellular Matrix Remodeling. In *The Guide to Investigation of Mouse Pregnancy*; Croy, B.A., Yamada, A.T., DeMayo, F.J., Adamson, S.L., Eds.; Academic Press: Boston, MA, USA, 2014; pp. 125–142.
45. Zhu, H.; Hou, C.C.; Luo, L.F.; Hu, Y.J.; Yang, W.X. Endometrial stromal cells and decidualized stromal cells: Origins, transformation and functions. *Gene* **2014**, *551*, 1–14. [[CrossRef](#)] [[PubMed](#)]
46. Iwahashi, M.; Muragaki, Y.; Ooshima, A.; Yamoto, M.; Nakano, R. Alterations in distribution and composition of the extracellular matrix during decidualization of the human endometrium. *Reproduction* **1996**, *108*, 147–155. [[CrossRef](#)]
47. Tsuno, A.; Nasu, K.; Yuge, A.; Matsumoto, H.; Nishida, M.; Narahara, H. Decidualization Attenuates the Contractility of Eutopic and Ectopic Endometrial Stromal Cells: Implications for Hormone Therapy of Endometriosis. *J. Clin. Endocrinol. Metab.* **2009**, *94*, 2516–2523. [[CrossRef](#)]
48. Gordiyenko, O.I.; Kovalenko, I.F.; Rogulska, O.Y.; Trufanova, N.A.; Gurina, T.M.; Trufanov, O.V.; Petrenko, O.Y. Theory-based cryopreservation mode of mesenchymal stromal cell spheroids. *Cryobiology* **2024**, *115*, 104906. [[CrossRef](#)]
49. Dong, H.; Li, X.; Chen, K.; Li, N.; Kagami, H. Cryopreserved Spontaneous Spheroids from Compact Bone-Derived Mesenchymal Stromal Cells for Bone Tissue Engineering. *Tissue Eng. Part C Methods* **2021**, *27*, 253–263. [[CrossRef](#)]
50. Li, Q.; Yuan, Y.; Zhao, W.; Li, Y.; Shi, J.; Xiu, Y.; Han, M.; Han, Y.; Zhang, J.; Cheng, S.; et al. A 3D in vitro model for studying human implantation and implantation failure. *Cell* **2026**, *189*, 70–86.e20. [[CrossRef](#)]
51. Huang, X.; Yang, X.; Huang, J.; Wei, L.; Mao, Y.; Li, C.; Zhang, Y.; Chen, Q.; Wu, S.; Xie, L.; et al. Correction: Human amnion mesenchymal stem cells promote endometrial repair via paracrine, preferentially than transdifferentiation. *Cell Commun. Signal.* **2024**, *22*, 326. [[CrossRef](#)]
52. Yamauchi, N. Development of a three-dimensional culture model of endometrium to study embryo-uterine interactions. *J. Reprod. Dev.* **2026**. Online ahead of print. [[CrossRef](#)]

**Disclaimer/Publisher’s Note:** The statements, opinions and data contained in all publications are solely those of the individual author(s) and contributor(s) and not of MDPI and/or the editor(s). MDPI and/or the editor(s) disclaim responsibility for any injury to people or property resulting from any ideas, methods, instructions or products referred to in the content.